Published in final edited form as:
Arterioscler Thromb Vasc Biol. 2011 December ; 31(12): 2889–2896. doi:10.1161/ATVBAHA.111.236570.

Spatial distribution and mechanical function of elastin in resistance arteries - a role in bearing longitudinal stress

Philip S. Clifford[1,2,*], **Srikanth R. Ella**[1,3,*], **Aaron J. Stupica**[1,3], **Zahra Nourian**[1], **Min Li**[1], **Luis A. Martinez-Lemus**[1,4], **Kim A. Dora**[5], **Yan Yang**[1], **Michael J. Davis**[1,3,4], **Ulrich Pohl**[6], **Gerald A. Meininger**[1,3,4,#], and **Michael A. Hill**[1,3,4,#]

[1]Dalton Cardiovascular Research Center, University of Missouri, Columbia, Missouri 65211

[2]Department of Anesthesiology, Medical College of Wisconsin and VA Medical Center, Milwaukee, WI 53295

[3]Department of Biological Engineering, University of Missouri, Columbia, Missouri 65211

[4]Department of Medical Pharmacology and Physiology, University of Missouri, Columbia, Missouri 65211

[5]Department of Pharmacology, University of Oxford, Oxford OX1 3QT, UK

[6]Walter-Brendel-Centre of Experimental Medicine, Ludwig-Maximilians-Universitaet Muenchen, Munich, Germany

Abstract

Objective—Despite the role that extracellular matrix (ECM) plays in vascular signaling, little is known of the complex structural arrangement between specific ECM proteins and vascular smooth muscle cells (VSMCs). Our objective was to examine the hypothesis that adventitial elastin fibers are dominant in vessels subject to longitudinal stretch.

Methods and Results—Cremaster muscle (CM) arterioles were isolated and allowed to develop spontaneous tone and compared with small cerebral arteries. 3D confocal microscopy was used to visualize ECM within the vessel wall. Pressurized arterioles were fixed and stained with: Alexa 633 Hydrazide (as a non-selective ECM marker), anti-elastin or anti-type 1 collagen antibody and a fluorescent nuclear stainExposure of CM arterioles to elastase for 5 min caused an irreversible lengthening of the vessel segment not observed in cerebral arteries. Longitudinal elastin fibers were demonstrated on CM arterioles using 3D imaging but were confirmed to be absent in cerebral vessels. The fibers were also distinct from type I collagen fibers and were degraded by elastase treatment.

Conclusion—These results indicate the importance of elastin in bearing longitudinal stress in the arteriolar wall and that these fibers constrain VSMCs. Differences between skeletal muscle and cerebral small arteries may reflect differences in the local mechanical environment such as exposure to longitudinal stretch.

Keywords

Extracellular matrix proteins; elastin; arteriole; resistance artery; mechanical properties; confocal imaging

[#]Authors for Correspondence: Michael A. Hill, Ph.D. and Gerald A. Meininger, Ph.D., Dalton Cardiovascular Research Center, University of Missouri, Columbia, MO 65211, Ph: 1-573-884-4601, hillmi@missouri.edu or meiningerg@missouri.edu.
[*]These Authors contributed equally to this work.

c. Disclosures: none.

INTRODUCTION

The extracellular matrix (ECM) contains a number of proteins including collagen, elastin, laminin, fibronectin, vitronectin, glycoproteins, and proteoglycans. In addition to providing a mechanically dynamic structural scaffold, the ECM is involved in physiological processes such as cell growth, differentiation, and migration. With respect to the vasculature, recent studies have demonstrated a number of these ECM proteins to actively signal through outside-in means into both vascular smooth muscle and endothelial cells, particularly conveying mechanical signals. For example, fibronectin binding through cell surface integrins modulates the activity of smooth muscle cell ion channels (voltage-gated Ca^{2+} channels and large conductance Ca^{2+}-activated K^+ channels)[1–3] and affects local cellular contractions [4]. Similarly, extracellular matrix protein – integrin activation of various intracellular signaling mechanisms underlies endothelial cell mechanotransduction to stimuli such as shear stress [5,6]. Despite these demonstrated roles of the extracellular matrix (ECM) in vascular cell signaling, relatively little is known of the complexities of the in situ arrangement between specific ECM proteins and arteriolar smooth muscle cells. Given the above examples, it is likely that the structural arrangement of the vessel wall ECM proteins, particularly at the microvascular level, impacts on how local mechanical forces are transmitted, sensed and responded to and, ultimately, how effectively a vessel is able to alter its diameter.

Adding to difficulties in understanding the complexity of the extracellular components of the vessel wall is an apparent regional heterogeneity. Importantly, regional differences involve both variation in matrix composition and structural arrangement. Thus, in contrast to skeletal muscle arterioles, small cerebral arteries lack an external elastic lamina that is present in many peripheral vessels [7]. Both vessel types exhibit an internal elastic lamina (IEL) although recent studies have suggested that heterogeneity at this level may underlie differences in myoendothelial gap junction (MEGJ)-mediated communication and functional responses mediated through hyperpolarization [8,9].

In regard to specific ECM proteins, Baumbach and colleagues have provided information on the composition of the arteriolar wall, particularly as it relates to the cerebral circulation under physiological conditions and in experimental models of hypertension[10–12]. Those studies have emphasized the significant contribution that elastin makes to the overall composition of the vessel wall. From a functional perspective, elastin is an important determinant of arterial distensibility, and hence stiffness, in conduit vessels. Elastin's contribution is particularly relevant at low intraluminal pressures as compared to collagen that exerts its effects on distensibility at higher pressures[13]. Despite this, the functional role of elastin in small arteries and arterioles is less well defined[14].

We hypothesized that an adventitial population of elastin-rich fibers exists in the vessel wall that are predominantly arranged in a longitudinal fashion and thereby bear and exert longitudinal mechanical stress in the arteriolar wall. To examine this hypothesis we predicted that abluminal exposure of isolated arterioles to elastase would cause vessel lengthening. Further, we predicted that this response to elastase would be absent in vessels lacking an overt external elastic lamina (such as small cerebral arteries).

MATERIALS AND METHODS

All studies were performed on arterial blood vessels obtained from male Sprague-Dawley rats (175 – 250 g; 6 – 9 weeks of age). Surgical and animal handling procedures were approved by the Animal Care and Use Committee of the University of Missouri.

Vessel Isolation, Cannulation and Study

Cremaster first order (1A) arterioles, small cerebral and mesenteric arteries were isolated from rats as previously described and cannulated for isobaric protocols [15, 16]; see Supplementary Material). Arterioles were exposed for 5 min to porcine pancreatic elastase (0.05 units/ml) then washed for 20 min. Vasomotor responses were then re-assessed. In some experiments vessels were superfused with a 0 mM Ca^{2+} physiological salt solution containing 2 mM EGTA to allow passive distensibility (pressure – diameter) relationships to be determined before and after elastase treatment. All elastase digestions were performed in the presence of a Ca^{2+}-containing physiological salt solution.

Imaging and 3D Reconstruction/Data Analysis

Pressurized arterioles were fixed (2% paraformaldehyde) and stained with: Alexa 633 Hydrazide (0.2 μM, Ex 633/Em 700nm; non-selective matrix staining dye), anti-elastin antibody (1° antibody dilution 1:100; 2° AB, 491/515nm) and a nuclear stain Yo-Pro-1 iodide (491/515nm) or 4′6-diamino-2-Phenylindol (DAPI, 500ng/ml, Ex: 355, Em: 400–450nm) [17]. A subset of vessels were stained for type I collagen using an anti-rat polyclonal antibody (Millipore; 1:1000, 1μg/ml) and a goat anti-rabbit Alexafluor 488 secondary antibody (20μg/ml).

3D confocal microscopy was used to visualize ECM within the arteriole wall. Imaging was performed using a Leica TCS-SP5 microscope in conjunction with a Leica 63X water immersion objective lens (NA 1.2) and Leica LAS AF image acquisition software. 512×512 pixel images were acquired at a resolution of 0.48 μm/pixel at 400 Hz. Line averaging (3 scans) was performed to reduce the low frequency noise. Z dimension step size was 0.05 – 0.3 μm for all z-stacks. All acquisitions represent 8-bit TIFF grey scale images. Post image acquisition analyses were performed using Image J (NIH, Bethesda, MD), Imaris (Bitplane Scientific Software, South Windsor, CT) and Image Pro (Media Cybernetics, Bethesda, MD).

See Supplement for detailed Materials and Methods including additional information relating to image acquisition and processing.

Chemicals and Reagents

Porcine elastase was obtained from Calbiochem (48 U/g; catalog # 324682; Lot # D00012477; EMD Chemicals, San Diego, CA) or from Sigma Chemical Company (5.9U/mg; catalog # E1250; Lot # 041M7018V; St Louis, MO). Type II collagenase (553 U/mg) was purchased from Sigma Chemical Company. Anti-elastin antibody was obtained from Chemicon International (Millipore, Billerica, MA) and anti-collagen antibody directly from Millipore (Billerica, MA). Species appropriate secondary antibodies were obtained from Molecular Probes (InVitrogen, Carlsbad, CA). Alexa Hydrazide, Yo-Pro-1 Iodide and DAPI were similarly obtained from Molecular Probes.

Statistical Methods

Results are presented as mean ± SEM. Simple comparisons between two means were performed using a two-tailed Student t-test while multiple group comparisons were performed using analysis of variance (ANOVA) with Tukey's *post hoc* test. Statistical significance was assumed at the $p < 0.05$ level.

RESULTS

Treatment of Cremaster Arterioles with Elastase Causes Irreversible Lengthening

After developing myogenic tone, cannulated and pressurized (70 mmHg) cremaster 1As were subjected to a 5 min exposure to elastase (0.05 U/ml) delivered to the adventitial surface. Length of vessels was assessed prior to enzyme exposure and again following elastase treatment (and 20 min washout) by adjusting the calibrated x translational direction of the micromanipulator holding the cannulation pipette. Lumenal diameter was monitored continually during elastase treatment and subsequent washout. The arterioles responded to the elastase by significantly lengthening by 35.6 ± 2.3% (n = 10; $p<0.05$) (Figure 1) while there was little apparent change in diameter (− 5.2 ± 0.8 %). The lengthening, evident as a lateral bowing of the vessel between the cannulation pipettes, was not reversed by washout of the elastase, consistent with a direct effect on the vessel structure. An example time course for the elastase-induced lengthening of a cremaster muscle arteriole is shown in Figure 1a and b.

Studies of reactivity were performed to demonstrate that the vessels retained viability and that cellular contractile function was intact. Vessels held pressure and did not display leaks. Further, vessels retained steady-state myogenic tone although acute myogenic reactivity was depressed (Figure 2a). No difference in ability to dilate to acetylcholine (10^{-6}M) or contract to phenylephrine (10^{-6}M) was observed (Figure 2b).

To assess the effects of elastase treatment on the passive properties of the cannulated cremaster arterioles, pressure-diameter (PD) relationships were measured after superfusion with physiological salt solution lacking Ca^{2+} and containing 2mM EGTA. Elastase caused a significant leftward shift in the PD relationship particularly at low pressures (Figure 2c) consistent with a major effect on the elastin components of the vessel wall as opposed to the collagen fibers[13, 14].

To quantify the degree of cremaster arteriole lengthening and to determine its effects on elements of the vessel wall, cell width and number of cells per unit length were determined pre- and post-elastase treatment. To facilitate these measurements a dye exclusion technique was used as previously described[18]. Cell impermeable DCF was placed in the vessel bath from where it subsequently diffused into the spaces between VSMCs. Acquired images are then digitally inverted to reveal the SMCs, which allowed cell shape to be readily discerned (see Supplementary Material Figure I). Cell width increased significantly ($p < 0.05$) following elastase treatment while the number of cells per unit length decreased significantly ($p < 0.05$) (Table 1). Lengthening was also associated with a change in shape of IEL holes as indicated by a significant ($p < 0.05$) increase in the long axis:short axis ratio (Table 1).

Since elastase is a serine protease it was considered conceivable that the lengthening effect may reflect an action on multiple ECM targets. As a comparison an additional set of cannulated vessels was similarly exposed to type II collagenase (30 Units/ml, 5 min). In contrast to elastase, vessels treated with collagenase did not lengthen but showed significant vasodilation (34.1 ± 4.0%; n=6; $p<0.05$; Figure 2d; **see** Supplementary Material Figure III for additional information). Also, in contrast to elastase treatment, the dilator effect of collagenase was reversed on washout (Figure 2d and **see** Supplementary Material).

In Contrast Small Cerebral Arteries Do Not Lengthen In Response to Elastase

In additional studies the effects of elastase treatment were compared between cerebral arteries (n = 8) and cremaster 1As (n = 8). Vessels (taken from the same animals) were cannulated and treated in a similar fashion and all developed spontaneous myogenic tone.

While cremaster vessels again showed a lengthening response, the cerebral vessels were largely unaffected by elastase treatment (Figure 3). Example images and the time course of elastin exposure are shown in Figure 1.

Despite the absence of lengthening of cerebral vessels following elastase treatment, their passive pressure-diameter relationships showed a leftward and upward shift (Figure 3) consistent with the enzyme treatment exerting distinct effects on the two vessel types.

In cerebral vessels, elastase treatment did not cause a measurable change in VSMC width or the number of cells per unit length (Table 1). Further, cerebral VSMC width and numbers of cells per unit length were not significantly different from those of cremaster VSMCs under control conditions (Table 1). IEL hole long:short axis ratio in cerebral arteries was unaffected by the elastase treatment (Table 1).

Cremaster Arterioles Show Longitudinal Adventitial Fibers That Contain Elastin And Are Degraded By Elastase

Cremaster 1A arterioles, stained with Alexa 633 hydrazide and counterstained for nuclei, showed longitudinally arranged adventitial (superficial) fibers that were branched in a dense and complex fashion forming a network traversing the circumference of the vessel (Figure 4A; Supplementary Movie Files 1 and 2; Supplementary Figures 4a and b). From the reconstructed cross-sectional view, it is clear that the cremaster 1A has both an internal and external ECM layer (Figure 4A). The internal layer resembles previous descriptions of the internal elastic lamina and exhibited holes that have previously been described to be sites where myoendothelial cell projections can be found [9, 17, 19] (see also Supplementary Figure IV). The Alexa 633 hydrazide-stained adventitial ECM structure was absent in small cerebral arteries, consistent with the previous observation that these vessels lack a defined external elastic lamina (Figure 4B and Supplementary Movie Files 3 and 4).

Under the imaging conditions used, autofluorescence of ECM proteins did not contribute greatly to the images of vessels stained with Alexa 633 hydrazide. Details of control experiments are shown in the Supplementary Material.

Staining with a specific elastin antibody showed overlap between its pattern and the structures stained by the Alexa hydrazide dye suggesting that the adventitial fibers observed in cremaster vessels indeed contain elastin (Figure 5, panels a, b and c). Under the imaging conditions used no fluorescence staining was detected when the elastin (primary) antibody was omitted (data not shown; also see Supplementary Material). Vessels treated with elastase showed only remnants of these fibers and ‘areas of indentation’ where the fibers had likely been positioned prior to enzyme treatment (Figure 5d). It should be noted that, consistent with the observations of [14], the conditions of the elastase treatment (addition to the adventitial surface, time of exposure and concentration/activity of enzyme) were such that while the adventitial fibers were disrupted the IEL remained largely intact.

Staining with a specific antibody for a Type 1 collagen showed an entirely different staining pattern to either Alexa 633 hydrazide or the elastin antibody (**see** Supplementary Material Figure V). In contrast, to the distinct adventitial fibers shown by Alexa 633/elastin antibody staining, Type 1 collagen stained in a ‘wavy, belt or strap-like’ manner. A similar distribution of collagen was confirmed from autofluorescence images as used by previous investigators[20] (data not shown).

Small Mesenteric Arteries Contain Adventitial Fibers Resembling Those of Cremaster Arterioles

On the basis of the above we hypothesized that elastin fibers support vessels prone to longitudinal stretch and as such predicted that small mesenteric arteries should contain an elastin fiber network more closely related to cremaster vessels than cerebral arteries. Similar to the cremaster vessels, small mesenteric arteries stained with Alexa 633 hydrazide and counterstained for nuclei showed longitudinally arranged adventitial (superficial) fibers that branched into a very dense and complex network traversing the adventitia (Figure 6 and Supplementary Movie Files 5 and 6).

DISCUSSION

Despite consisting of only a few cell layers in thickness the walls of small arteries and arterioles present a complex biomechanical structure. Further, as a contractile tissue there is considerable interdependence of structure and cell function. Using confocal microscopy and 3 D imaging approaches to reconstruct through-focus structural features of the vascular wall, the present study illustrates the complexity of the ECM while also demonstrating that particular matrix proteins may constrain or shield the environment within which smooth muscle cells reside and exert their contractile activity. In this regard the data support a significant role for elastin-containing fibers in the mechanical properties of true resistance vessels [14] and suggest that this property is not limited to larger conduit vessels. These conclusions are highlighted by brief elastase treatment causing degradation of adventitial matrix fibers and significant lengthening of cremaster muscle arterioles. Heterogeneity between vascular beds was, however, also observed. In particular, small cerebral arteries that are known to lack an EEL [7] did not show lengthening to a similar elastase exposure.

In regard to the physiological significance of the apparent difference between adventitial structure of cremaster muscle and mesenteric arterioles versus small cerebral arteries, we speculate that this structure confers the ability to withstand longitudinal stretch. Thus, retraction and relaxation of the cremaster muscle would result in the centrally-located arteriole being subjected to longitudinally directed strain while cerebral vessels, located within a rigid skull, are largely protected from such elongation. To support this hypothesis mesenteric arteries were examined as another vascular bed where vessels are commonly subjected to longitudinal changes in length. Similar to the cremaster 1A, small mesenteric arteries also showed a complex network of adventitial matrix protein fibers. Supporting structural heterogeneity within the vessel wall (in particular as relates to the ECM) between vascular beds, elastin mRNA expression was significantly greater in cremaster and mesenteric vessels compared to small cerebral arteries. Further supporting heterogeneity the relative amount of muscle cell protein (measured as α actin content) was greater in cerebral arteries as compared to both cremaster and mesenteric vessels (see Supplementary Material Figure VI). Conceivably, morphological differences could also exist at the level of the VSMCs, however, under control conditions calculations of VSMC width and number of cells per unit length showed no differences between cremaster and cerebral small arteries.

Interestingly, although elastase did not cause lengthening of the small cerebral arteries both cremaster and cerebral vessels showed shifts in their passive pressure – diameter relationships on enzyme treatment. We speculate that this may be explained by differences in the longitudinal and circumferential properties of the vessel wall. Thus, the length changes are a function of the longitudinally arranged adventitial elastin fibers while the shifts in the pressure – diameter relationships may relate to effects of elastase on other elements such as the internal elastic lamina.

IEL holes have recently received considerable attention as sites of endothelial – smooth muscle cell connectivity via myoendothelial junctions[8, 19]. Additional analysis was undertaken to determine whether the elastase treatment affected the shape of IEL holes. To quantify changes the long axis:short axis ratio of the holes were determined. For measurement of the IEL hole size, the vessel image stacks were processed to extract the image data associated with IEL layer alone. Elastase treatment of cremaster vessels led to a significant ($p < 0.05$) increase in the long:short axis ratio of the IEL holes as the vessel lengthened. This could reflect either stretch of the IEL or a direct effect of the elastase on the IEL. In contrast to the cremaster arterioles, cerebral vessels neither lengthened nor changed the measured characteristics of the IEL holes. Indirectly, this supports the idea that cremaster arterioles are normally constrained in the axial direction by adventitially-located elastin fibers. Cleavage of these fibers leads an overt increase in vessel length, an increase in cell width and a stretching of wall structures such as the IEL.

The present studies did not consider any structural role played by other elements that contribute to the adventitia. Images stained with either DAPI or propidium iodide showed nuclei in the region of the adventita. In addition, the orientation of these cells indicated that they were unlikely to be either smooth muscle or endothelial cells. As these cells were apparent in cremaster vessels before and after elastase treatment (data not shown) it is unlikely that these elements contributed to the lengthening process. Nevertheless, future studies should be aimed at identifying the nature of such cells.

Consistent with elastase causing lengthening of the cremaster arteriole, arterial tortuosity has been reported in studies administering elastase in vivo to induce aneurysm formation[21–23] and in transgenic animal models where elastin levels are genetically manipulated[24]. Such studies have largely focused on conduit vessels due to the role of elastin in elastic recoil of arteries and the clinical significance of large vessel aneurysms. In addition to common findings with respect to vessel length, disruption of elastin appears to decrease the distensibility of both large arteries and, at least, first order arterioles from skeletal muscle. Also consistent with a role for elastin in regulating small vessel dimensions Briones et al.[14] showed elastase treatment to decrease the ex vivo distensibility of small mesenteric arteries. Interestingly, in the present imaging studies mesenteric vessels exhibited a complex adventitial fibrillar network similar to that observed in the walls of the cremaster muscle arterioles.

Additional studies will be required to delineate the exact involvement of specific matrix proteins. We initially used Alexa 633 hydrazide staining as a non-selective marker for extracellular matrix proteins. However, it is evident from the specific elastin staining that this dye preferentially binds elastin-containing structures. Further supporting its restricted staining was the observation that a different staining pattern is observed with an antibody known to be specific for Type 1 collagen. Similarly, cleavage of the fibers with elastase led to a leftward shift in the passive pressure-diameter relationship (for cremaster arterioles) at low pressures, consistent with the contribution of elastin to vascular mechanics as compared to that of collagen[13, 14]. This, however, does not indicate that the stained adventitial fibers are comprised of elastin alone and presumably contain other proteins such as fibrillin[24–26].

A question that arose from the present studies is whether or not the staining pattern of elastin-containing fibers found in the cremaster arterioles is representative of small arteries and arterioles in other skeletal muscles. Relevant to this, we have observed a complex fiber network in arterioles isolated from hamster gracilis muscle suggesting that a similar structure exists in differing skeletal muscles and across species (data not shown).

Important questions arising from our studies include how do VSMCs interact with the matrix scaffold and do the differences in regional matrix structure imply differences in how local mechanical forces are transmitted, sensed and responded to? Clearly, the lengthening of cremaster muscle 1As, and increasing SMC width, following elastase exposure suggests that under resting conditions smooth muscle cells are constrained along the long axis of the vessel or across the short axis of individual smooth muscle cells. Importantly, the enzyme treatment did not markedly alter vascular reactivity to vasoactive agents (acetylcholine and phenylephrine) and the vessels remained free of leaks to the intraluminal pressure. Further, while the lengthening response was seen with elastase treatment this was not seen following collagenase exposure. As such we do not believe that our observations can be simply explained by nonselective destruction of vessel integrity, per se.

In an earlier study, Spofford and Chilian[27] reported differing responses of cerebral and mesenteric small arteries with respect to pressure-induced changes in c-fos expression. Increasing intraluminal pressure led to a decrease in cerebral vessel c-fos expression while causing an increase in mesenteric vessels. Interestingly the pressure-induced effect on c-fos expression was mediated through the elastin-laminin receptor and could be blocked by decoy peptides that are presumed to inhibit normal matrix protein binding to elastin. These authors further found differences in the matrix protein composition between the cerebral and mesenteric vessels suggesting that the differences in pressure responsiveness may reflect regional variation in the matrix environment. Specifically, consistent with the present study, these authors reported an absence of elastin in the adventitia of the cerebral vessels and a presence of elastin in the adventitia of mesenteric vessels. Cerebral vessels, however, were reported to show comparatively greater levels of elastin within the medial layer.

In addition to understanding the physiological structure of the vessel wall the relevance to pathophysiology should also be noted. Although currently largely limited to studies of conduit vessels and sub-cutaneous resistance arteries, age-related changes in the ratio of elastin to collagen affects vascular stiffness[28–31]. Further, in aging and metabolic disturbances (for example in diabetes mellitus) long-lived proteins such as elastin and collagen are subject to modification by glycation and oxidation[32, 33]. Presumably such changes may alter not only the mechanical properties of the ECM proteins but also the relationship between the extracellular matrix and cellular elements of the vessel wall thus potentially affecting matrix protein-mediated cellular signaling.

Collectively, the data support our hypothesis that elastin is an important ECM protein for bearing longitudinal stress in the arteriolar wall. Further, when present, these fibers act to constrain or restrict the longitudinal dimensions of the vessel. Differences between arterioles from skeletal muscle and mesentery versus small arteries from the cerebral circulation may be related to differences in the local mechanical environments in which these vessels reside. Skeletal muscle and mesenteric tissues are continuously exposed to longitudinally oriented stretching forces that are transferred to the vasculature. By comparison, cerebral tissue is encapsulated and the brain vasculature is not normally exposed to these types of stretching forces. Knowledge of the 3D architecture of the extracellular matrix components of the vessel wall is also of importance to our understanding of how these elements are affected in aging and disease states particularly where matrix proteins are damaged, degraded [34] or post-translationally modified [32, 33].

Supplementary Material

Refer to Web version on PubMed Central for supplementary material.

Acknowledgments

a. Acknowledgements: none. ***b. Sources of Funding:*** studies described in this manuscript were supported by NIH grants to MAH (HL92241-02), GAM and MJD (P01 HL-095486), and LML (HL088105-02). PSC was supported by a Research Career Enhancement Award from the American Physiological Society.

References

1. Gui P, Chao JT, Wu X, Yang Y, Davis GE, Davis MJ. Coordinated regulation of vascular ca2+ and k+ channels by integrin signaling. Adv Exp Med Biol. 2010; 674:69–79. [PubMed: 20549941]
2. Wu X, Yang Y, Gui P, Sohma Y, Meininger GA, Davis GE, Braun AP, Davis MJ. Potentiation of large conductance, ca2+-activated k+ (bk) channels by alpha5beta1 integrin activation in arteriolar smooth muscle. J Physiol. 2008; 586:1699–1713. [PubMed: 18218680]
3. Yang Y, Wu X, Gui P, Wu J, Sheng JZ, Ling S, Braun AP, Davis GE, Davis MJ. {alpha}5{beta}1 integrin engagement increases bk channel current and ca2+ sensitivity through c-src mediated channel phosphorylation. J Biol Chem. 2009
4. Sun Z, Martinez-Lemus LA, Hill MA, Meininger GA. Extracellular matrix-specific focal adhesions in vascular smooth muscle produce mechanically active adhesion sites. Am J Physiol Cell Physiol. 2008; 295:C268–278. [PubMed: 18495809]
5. Shyy JY, Chien S. Role of integrins in endothelial mechanosensing of shear stress. Circ Res. 2002; 91:769–775. [PubMed: 12411390]
6. Alon R, Ley K. Cells on the run: Shear-regulated integrin activation in leukocyte rolling and arrest on endothelial cells. Curr Opin Cell Biol. 2008; 20:525–532. [PubMed: 18499427]
7. Lee RM. Morphology of cerebral arteries. Pharmacol Ther. 1995; 66:149–173. [PubMed: 7630927]
8. Sandow SL, Gzik DJ, Lee RM. Arterial internal elastic lamina holes: Relationship to function? J Anat. 2009; 214:258–266. [PubMed: 19207987]
9. Sandow SL, Haddock RE, Hill CE, Chadha PS, Kerr PM, Welsh DG, Plane F. What's where and why at a vascular myoendothelial microdomain signalling complex. Clin Exp Pharmacol Physiol. 2009; 36:67–76. [PubMed: 19018806]
10. Hajdu MA, Heistad DD, Siems JE, Baumbach GL. Effects of aging on mechanics and composition of cerebral arterioles in rats. Circ Res. 1990; 66:1747–1754. [PubMed: 2344672]
11. Baumbach GL, Hajdu MA. Mechanics and composition of cerebral arterioles in renal and spontaneously hypertensive rats. Hypertension. 1993; 21:816–826. [PubMed: 8500863]
12. Hajdu MA, Heistad DD, Ghoneim S, Baumbach GL. Effects of antihypertensive treatment on composition of cerebral arterioles. Hypertension. 1991; 18:II15–21. [PubMed: 1833321]
13. Dobrin PB. Mechanical properties of arterises. Physiol Rev. 1978; 58:397–460. [PubMed: 347471]
14. Briones AM, Gonzalez JM, Somoza B, Giraldo J, Daly CJ, Vila E, Gonzalez MC, McGrath JC, Arribas SM. Role of elastin in spontaneously hypertensive rat small mesenteric artery remodelling. J Physiol. 2003; 552:185–195. [PubMed: 12844513]
15. Hill MA, Zou H, Davis MJ, Potocnik SJ, Price S. Transient increases in diameter and [ca(2+)](i) are not obligatory for myogenic constriction. Am J Physiol Heart Circ Physiol. 2000; 278:H345–352. [PubMed: 10666063]
16. Meininger GA, Zawieja DC, Falcone JC, Hill MA, Davey JP. Calcium measurement in isolated arterioles during myogenic and agonist stimulation. Am J Physiol. 1991; 261:H950–959. [PubMed: 1887938]
17. Kansui Y, Garland CJ, Dora KA. Enhanced spontaneous ca2+ events in endothelial cells reflect signalling through myoendothelial gap junctions in pressurized mesenteric arteries. Cell Calcium. 2008; 44:135–146. [PubMed: 18191200]
18. Martinez-Lemus LA, Hill MA, Bolz SS, Pohl U, Meininger GA. Acute mechanoadaptation of vascular smooth muscle cells in response to continuous arteriolar vasoconstriction: Implications for functional remodeling. Faseb J. 2004; 18:708–710. [PubMed: 14977879]
19. Sandow SL, Neylon CB, Chen MX, Garland CJ. Spatial separation of endothelial small-and intermediate-conductance calcium-activated potassium channels (k(ca)) and connexins: Possible relationship to vasodilator function? J Anat. 2006; 209:689–698. [PubMed: 17062025]

20. Lee WK, Bell J, Kilpatrick E, Hayes M, Lindop GB, Dominiczak MH. Collagen-linked fluorescence in human atherosclerotic plaques. Atherosclerosis. 1993; 98:219–227. [PubMed: 8457261]
21. Dobrin PB, Mrkvicka R. Failure of elastin or collagen as possible critical connective tissue alterations underlying aneurysmal dilatation. Cardiovasc Surg. 1994; 2:484–488. [PubMed: 7953454]
22. Sasaki K, Ujiie H, Higa T, Hori T, Shinya N, Uchida T. Rabbit aneurysm model mediated by the application of elastase. Neurol Med Chir (Tokyo). 2004; 44:467–473. discussion 473–464. [PubMed: 15600281]
23. Azuma J, Maegdefessel L, Kitagawa T, Dalman RL, McConnell MV, Tsao PS. Assessment of elastase-induced murine abdominal aortic aneurysms: Comparison of ultrasound imaging with in situ video microscopy. J Biomed Biotechnol. 2011; 2011:252141. [PubMed: 21331328]
24. Carta L, Wagenseil JE, Knutsen RH, Mariko B, Faury G, Davis EC, Starcher B, Mecham RP, Ramirez F. Discrete contributions of elastic fiber components to arterial development and mechanical compliance. Arterioscler Thromb Vasc Biol. 2009; 29:2083–2089. [PubMed: 19850904]
25. Wagenseil JE, Mecham RP. New insights into elastic fiber assembly. Birth Defects Res C Embryo Today. 2007; 81:229–240. [PubMed: 18228265]
26. Mariko B, Pezet M, Escoubet B, Bouillot S, Andrieu JP, Starcher B, Quaglino D, Jacob MP, Huber P, Ramirez F, Faury G. Fibrillin-1 genetic deficiency leads to pathological ageing of arteries in mice. J Pathol. 2011; 224:33–44. [PubMed: 21432852]
27. Spofford CM, Chilian WM. Mechanotransduction via the elastin-laminin receptor (elr) in resistance arteries. J Biomech. 2003; 36:645–652. [PubMed: 12694994]
28. Cox RH. Age-related changes in arterial wall mechanics and composition of nia fischer rats. Mech Ageing Dev. 1983; 23:21–36. [PubMed: 6656298]
29. Gaballa MA, Jacob CT, Raya TE, Liu J, Simon B, Goldman S. Large artery remodeling during aging: Biaxial passive and active stiffness. Hypertension. 1998; 32:437–443. [PubMed: 9740608]
30. Intengan HD, Deng LY, Li JS, Schiffrin EL. Mechanics and composition of human subcutaneous resistance arteries in essential hypertension. Hypertension. 1999; 33:569–574. [PubMed: 9931167]
31. Intengan HD, Thibault G, Li JS, Schiffrin EL. Resistance artery mechanics, structure, and extracellular components in spontaneously hypertensive rats: Effects of angiotensin receptor antagonism and converting enzyme inhibition. Circulation. 1999; 100:2267–2275. [PubMed: 10578002]
32. Akhtar K, Broekelmann TJ, Miao M, Keeley FW, Starcher BC, Pierce RA, Mecham RP, Adair-Kirk TL. Oxidative and nitrosative modifications of tropoelastin prevent elastic fiber assembly in vitro. J Biol Chem. 2010; 285:37396–37404. [PubMed: 20847053]
33. Konova E, Baydanoff S, Atanasova M, Velkova A. Age-related changes in the glycation of human aortic elastin. Exp Gerontol. 2004; 39:249–254. [PubMed: 15036419]
34. Brooke BS, Bayes-Genis A, Li DY. New insights into elastin and vascular disease. Trends Cardiovasc Med. 2003; 13:176–181. [PubMed: 12837579]

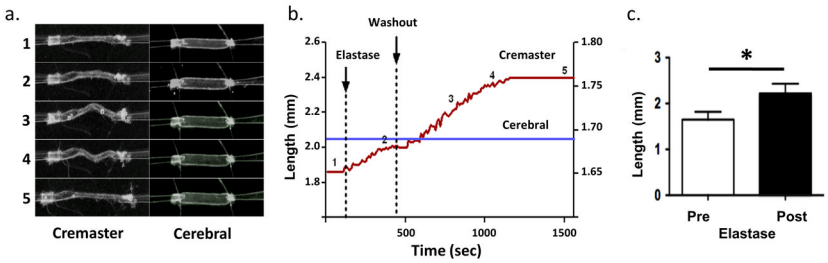

Figure 1.

Effect of elastase treatment on the length of cannulated cremaster and cerebral small arteries. **Panel a** shows example images for a cremaster and cerebral vessel. The numbers 1–5 refer to specific time-points as shown in **Panel b.** Note that the cremaster vessel shows considerable lengthening while the cerebral vessel is relatively unaffected. Note also that in image 5 for the cremaster vessel the pipettes have been repositioned in the 'x' dimension to straighten the vessel. Images were collected in real-time using a stereomicroscope coupled to a CCD camera and digital video recorder. Avi files were subsequently imported into Image Pro software for continuous measurement of vessel length. Length of the cremaster vessel is shown on the left hand y-axis and the cerebral artery on the right hand axis. **Panel c,** group data showing that abluminal application of elastaste (0.05 U/ml, 5 min) led to a significant ($p<0.05$) increase in cremaster vessel segment length ($n = 10$).

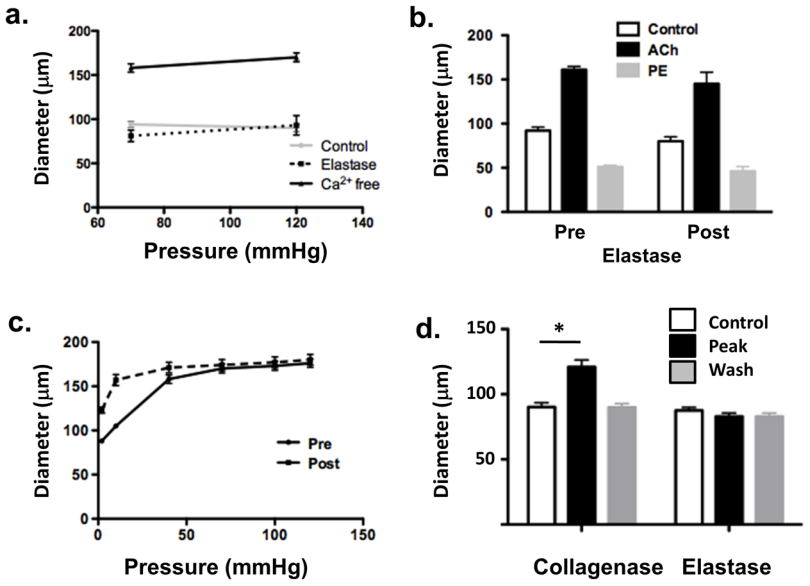

Figure 2.

Panel a, following elastase treatment vessels continued to show pressure-induced myogenic tone (left) although acute myogenic responsiveness was blunted (right). **Panel b**, following elastase treatment vessels (n = 6) showed dilation to ACh (10^{-6} M) and constriction to phenylephrine (10^{-6} M) (right) comparable to that under control conditions (left). **Panel c**, elastase treatment caused a leftward shift in the passive pressure – diameter relationship compared to baseline indicating an increase in vessel stiffness. **Panel d** - collagenase treatment caused dilation of myogenically active cremaster arterioles (n = 6). This effect was reversed by washing and was in contrast to the effect of elastase which caused irreversible lengthening of the cannulated vessel segments. Results are shown as mean ± SEM, * $P < 0.05$.

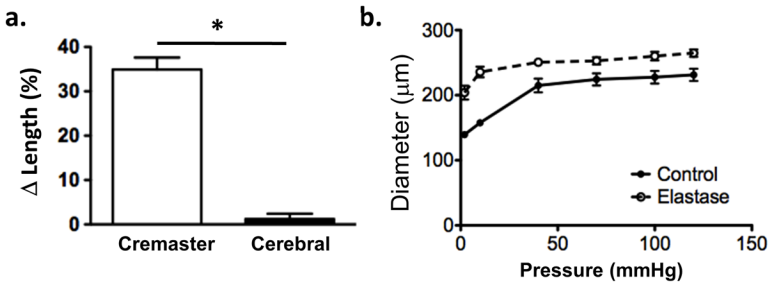

Figure 3.

Panel a, elastase treatment (0.05 U/ml; 5 mins) does not cause lengthening of cerebral arteries (n = 8) despite causing lengthening of cremaster arterioles (n = 8). **Panel b**, elastase treatment causes an upward and leftward shift in the passive pressure – diameter relationship for cerebral vessels showing a decrease in distensibility (n = 6). Results are shown as mean ± SEM. * $P < 0.05$.

Figure 4a

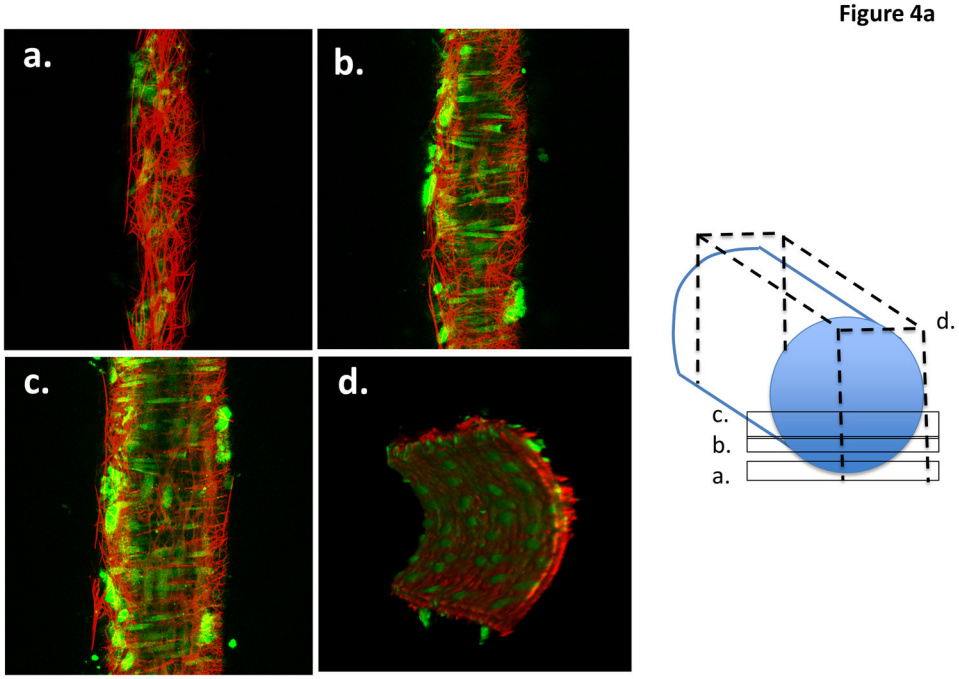

Figure 4b

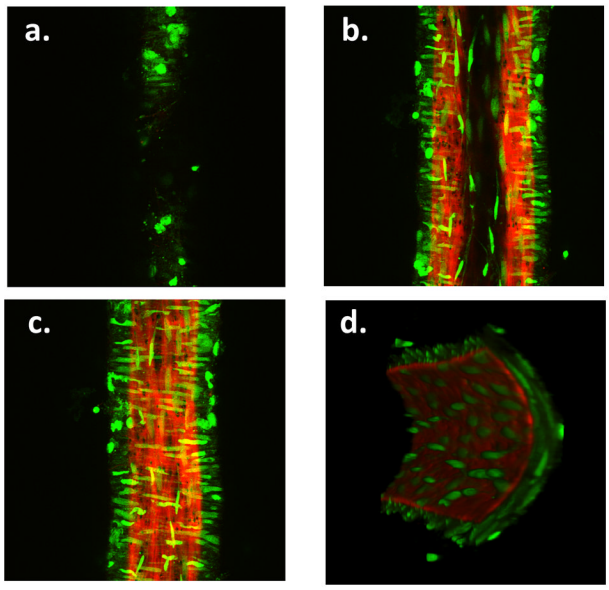

Figure 4.

Example pseudocolored images of a cannulated and pressurized cremaster arteriole (A) and a similarly prepared small cerebral artery (B). The images represent adventitial (**Panel a**), mid-wall (**Panel b**) intimal (**Panel c**) and end view **(Panel D)** sections. Vessel segments were fixed while pressurized (see text for details) and stained with Alexa 633 (for ECM structures) and Yo-Pro-1 iodide (nuclei). Images are representative of n = 11 (cremaster) and 6 (cerebral). Movie files for the complete image stacks and 3D rotating representations are shown in the Supplementary Material.

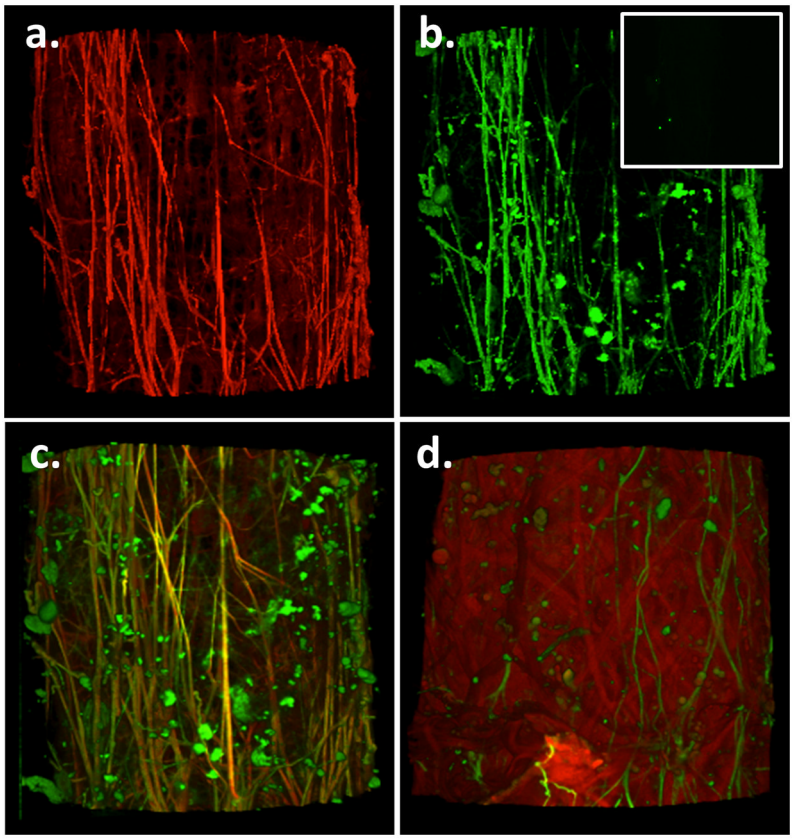

Figure 5.

Panel a shows Alexa 633 hydrazide staining of adventitial fibers in a cannulated cremaster 1A segment. **Panel b** shows the same vessel segment stained with a specific elastin antibody and a secondary antibody conjugated with Alexa fluor 488. Insert shows secondary antibody only control (additional details of controls are provided in the Supplementary Material). **Panel c** shows the overlay image for panels a and b. Results are typical of n = 4. Yellow color indicates apparent colocalization suggesting that the Alexa 633 hydrazide stained fibers contain elastin. **Panel d** elastase (0.05 U/ml, 5 min) cuts the longitudinally arranged, elastin-containing fibers (typical of n = 3).

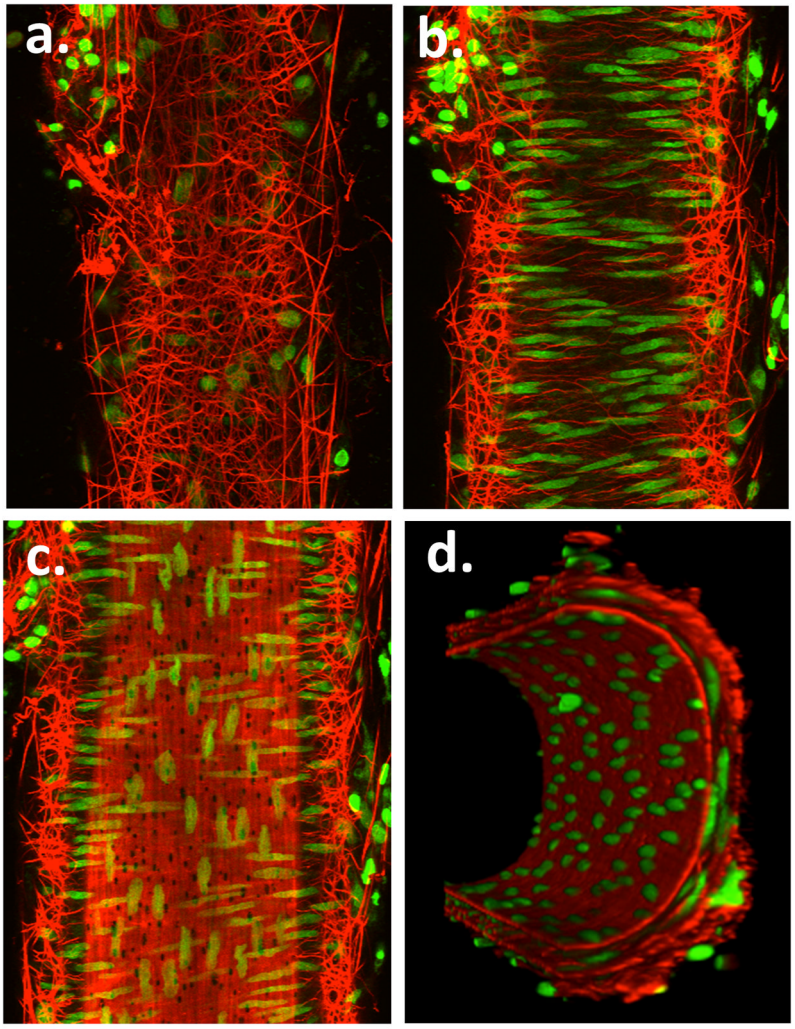

Figure 6.
Example pseudocolored images showing adventitial (**Panel a**), mid-wall (**Panel b**) intimal (**Panel c**) and end view (**Panel d**) sections of a small cannulated mesenteric artery. Vessel segments were fixed while pressurized and stained with Alexa 633 (for ECM structures) and Yo-Pro-1 iodide (nuclei). Images are representative of n = 3 vessels. Movie files for the complete image stacks and 3D rotating representations are shown in the Supplementary Material.

Table 1

Quantitative analyses of the effects of elastin treatment on VSMCs and IEL.

	Cremaster Arterioles		Small cerebral Arteries	
	Control (n =4)[†]	**+ Elastase (n =4)**	**Control (n =3)**	**+ Elastase (n =3)**
SMC width	5.64 ± 0.06	6.98 ± 0.10 *	5.67 ± 0.13	5.91 ± 0.12
SMC number/unit length[††]	34.0 ± 1.6	30.3 ± 1.2 *	33.0 ± 1.5	32.7 ± 1.7
IEL Holes (Long:short axis)[†††]	2.56 ± 0.52	3.63 ± 0.39 *	1.70 ± 0.17	1.77 ± 0.14

* $p < 0.05$ compared to respective control value

† n = number of vessels. For each vessel, measurements are based on approximately 30 SMCs as noted in the Table. Due to differences in the distribution of IEL hole numbers between vessel types, measurements of long:short axis ratios are based on an average of 24 holes/cremaster veseel and 13 holes/cerebral artery.

†† unit length = 134 μm

††† Long axis:short axis ratio as a measurement of IEL hole shape